Dissolution features on diamonds from hypabyssal kimberlite facies and the effect of melt composition on diamond resorption

by

Rosa Toutah

Submitted in partial fulfillment of the requirements for the degree of Bachelor of Science in

Earth Sciences and Chemistry

at

Dalhousie University

Halifax, Nova Scotia

April 2022

Supervisor: Dr. Yana Fedortchouk

Table of Contents

List of Figures

List of Tables

Abstract

Diamonds can preserve features from their time deep in earth's mantle and their ascent from the mantle to the Earth's surface in hot kimberlite magma due to their high stability. The record of dissolution textures on diamond surfaces opens a window into the history of the diamonds journey through the kimberlite. Composition of kimberlitic fluid affects dissolution textures on diamonds from volcaniclastic kimberlite facies. The focus of this study is to identify different resorption styles of diamonds from hypabyssal kimberlite facies and use experiments in volatile-undersaturated melt to determine the effect of melt composition on diamond resorption features. The study uses 1300 diamonds from 16 kimberlites from the Ekati Mine, selected hypabyssal dykes, and sills. This data obtained for class 3 kimberlites will be compared to the existing data on diamonds from class 1 kimberlites. SEM, AFM and microscope imaging will be utilized for analysis of surface features. Secondary dissolution corrosion sculpture (CS) features seen on tetrahexahedra (THH) diamond faces will act as a proxy for kimberlite melt composition to allow for the identification of kimberlitic conditions in class 1 and 3 hypabyssal kimberlites. Experiments in a Piston-cylinder apparatus will quantify the effect of melt composition and temperature/pressure variation on the diamond dissolution features. The experiments are conducted between 1000-1200ºC in silicate, carbonate, and silicate-carbonate melts at 1 GPa in "dry" or H2O-undersaturated conditions. Experiments done in exact temperature pressure conditions with either silicate or carbonate melts have shown drastic differences in resorption styles and features. Diamonds in silicate rich melts under 1 GPa of pressure at 1100 ºC demonstrate strong resorption on the {111} and {012} faces whereas the same experiment in a carbonate melt demonstrates strong graphitization and little resorption. The established relationship between dissolution features on diamonds and composition of kimberlitic melt will allow a long-standing question to be addressed, if different kimberlite classes are formed by a uniform kimberlite melt due to difference in the country rock characteristics or due to compositional differences in kimberlite melt. In addition, use of surface features on microdiamonds from hypabyssal kimberlite facies for early identification of kimberlite class will help better planning for drilling programs and diamond grade assessment. This allows for saving on drilling costs and improves the modelling of kimberlite emplacement.

KEYWORDS: Kimberlites; Hypabyssal; Diamonds; Dissolution features; Kimberlitic Melt

Chapter 1: Introduction

1.1 Objective of this study

Kimberlite pipes and kimberlitic processes are currently the most common source of diamonds in the world. The goal of this study is to use diamond dissolution features to help investigate and analyze kimberlitic emplacement conditions with the purpose of efficient kimberlite identification. By utilizing the method proposed in Fedortchouk (2007) diamond surface features can indicate the composition of late magmatic kimberlitic fluid and volatile behaviour (Fedortchouk, 2010). Free fluids dominated by hydrogen, carbon, and oxygen give rise to dissolution patterns more common in natural diamonds, whereas fluid-undersaturated kimberlite melts gives rise to surface graphitization, irregular cavities, and sharp features, which is not common and even rare in natural diamonds (Tolansky, 1968; Wagner, 1914). Features seen on a diamond from a carbonate rich melt between pressures of 1-7 GPa and 1150-1350C, include preservation of octahedron shape, {111} faces keeping trigonal contour, lots of trigon etching, pointed bottoms, hexagonal pits, and the erasing of pre-existing feature on the diamond face and developing specific irregular patterns (Fedortchouk, 2010). This evidence indicates there is a clear correlation between melt composition/experimental conditions and the type/style of resorption features on the diamond surface. Now with this study, we hope to use this correlation of melt to dissolution features to predict kimberlite class from hypabyssal diamonds. Diamonds from hypabyssal facies of class one intrusive/extrusive kimberlites have different surface features than diamonds from the same lithology in class three infilled kimberlites (Fedortchouk 2017; 2010; Gurney 2004). Meaning diamond surface features from the hypabyssal lithology could be used as early identifiers for a kimberlite pipe.

1.2 Diamond and Surface Feature Classification

Natural diamonds come in many colors, shapes, and sizes. Kimberlitic diamonds from differing emplacement environments give rise to a variety of shapes, surface features, sizes, carats, and clarity (Fedortchouk, 2007;2019, Gurney 2004). Diamond features can vary greatly, even within the bounds of a single property (Gurney 2004).

Based on initial growth conditions, diamonds can be classified into three groups: monocrystalline growth, polycrystalline growth, and as a single crystal transitioning into polycrystalline growth (Sungawa, 1984). Monocrystalline diamonds commonly occur as cubes,

octahedrons, or rhombic dodecahedrons because of slower growth rates as single crystals (Tappert and Tappert, 2011). Polycrystalline growth is the result of the fastest growth rate and creates aggregates of diamonds (Tappert and Tappert, 2011).

Early diamond morphology, based on the growth conditions, is denoted as a primary feature. Primary features are characteristically sharp and occur during initial crystallization in the mantle (Fedortchouk, 2019). Any subsequent growth or changes in the diamond crystal lattice is classified as a secondary feature (Fedortchouk, 2019).

Secondary features occur either immediately after the crystallization of the diamond, or during the diamond's ascent through the kimberlite pipe. These features are characteristically rounder and less sharp (Fedortchouk, 2019). Kimberlitic resorption from partial dissolution could lead to eventual tetrahexahedra (THH) or dodecahedron morphology (Fedortchouk, 2019). When describing rounded monocrystalline diamonds having undergone kimberlitic resorption there are two categories for which they can be placed into, a THH or dodecahedron (Fedortchouk, 2019). THH morphology is described as a diamond with 24 curved faces and dodecahedron morphology is described as a diamond with 12 curved faces (Fedortchouk, 2019). THH morphology will develop from a ditrigonal shape, and a dodecahedron morphology develops from a trigonal face, as seen in figure 1.1.1. As it is more common in natural samples, THH morphology will be utilized as criteria for diamond selection in this study, see chapter 2.

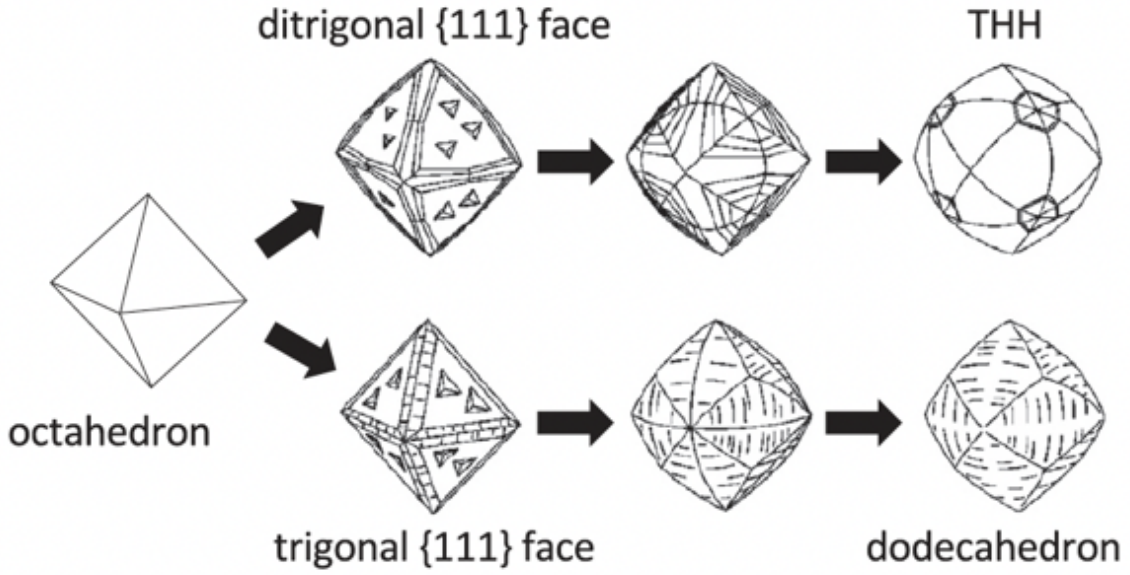

Figure 1.1.1: Evolution of octahedral diamond morphology from secondary growth, based on face shape. (Fedortchouk, 2019)

Different secondary surface features will develop based on their location on the diamond. The three locations denoted are the three crystallographic directions of a diamond lattice, the octahedra {111}, cubic {100}, and THH {012}, different resorption features will develop on each, as seen in figure 1.1.2 (Fedortchouk, 2019). Depending on the feature, it will either preferentially develop on only one diamond face, or develop on multiple faces (Fedortchouk, 2019). On the octahedra face {111} there is etch pit development, such as trigons, hexagons, and irregular laminae (Fedortchouk, 2019). Trigons are triangular pits created during the dissolution, described as either positive or negative, a positive trigon will have two adjacent sides parallel to the diamond edges and a negative trigon will have its point perpendicular to the diamond edge (Fedortchouk, 2019). The shape and number of trigons is correlated to their conditions of resorptions, which furthers the point that dissolution conditions have an impact on resorption style (Fedortchouk, 2007). Dissolution conditions high in H_2O will give rise to flat-bottomed trigons, whereas an increase in CO_2 will cause an increase in the size of pointed-bottom trigons (Fedortchouk, 2007). Hexagons occur when a pit develops both positive and negative walls (Fedortchouk, 2019). Lamellae develop during either growth or resorption, if a result of growth they will be thick step-faces with a triangular shape and sharp edges, if a result of resorption they will be thick step-faces, with an irregular outline and rounded edges (Fedortchouk, 2019). On the cubic face {100} there will be tetragonal pit development, either as negative square pits or positive square pits (Fedortchouk, 2019), although these will not be further studied in this paper as they were not observed in any natural or experimental diamonds. On the THH face {012} there is hillocks, terraces and circular pits which can develop (Fedortchouk, 2019). Hillocks are dissolution-based growths on the diamond surface whose shape is dependent on the diamond crystal lattice, they are shorter and more drop-like near the apices and more elongated near the edges (Fedortchouk, 2019). Terraces are step-like facies which grow and stack upon each other, typically along diamond edges and are seen with endings that resemble hillocks (Fedortchouk, 2019). Of the features described the focus of this studies dissolution feature characterization will be on trigons, terraces (figure 1.1.3a), cavities/pits (figure 1.1.3b), and hillocks (figure 1.1.4).

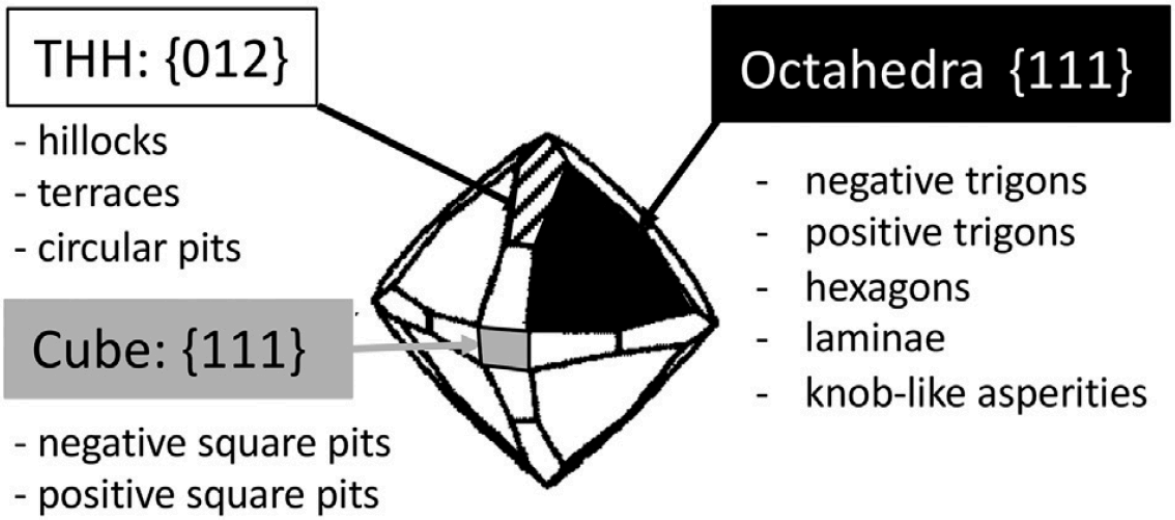

Figure 1.1.2: Three diamond lattice crystallographic directions, and subsequent resorption features each direction will develop into (Fedortchouk, 2019).

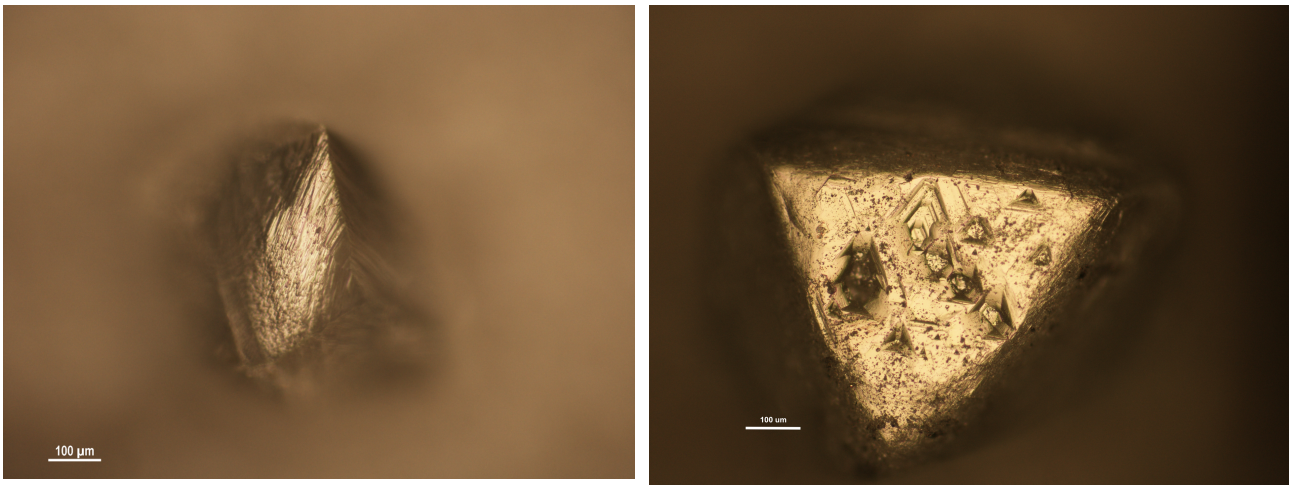

Figure 1.1.3: Image on left demonstrates the development of terraces along experimental diamond RT-2, image on the right shows deep cavity and pit development on experimental diamond RT-7, both imaged under a petrographic micrscope at 10x magnification.

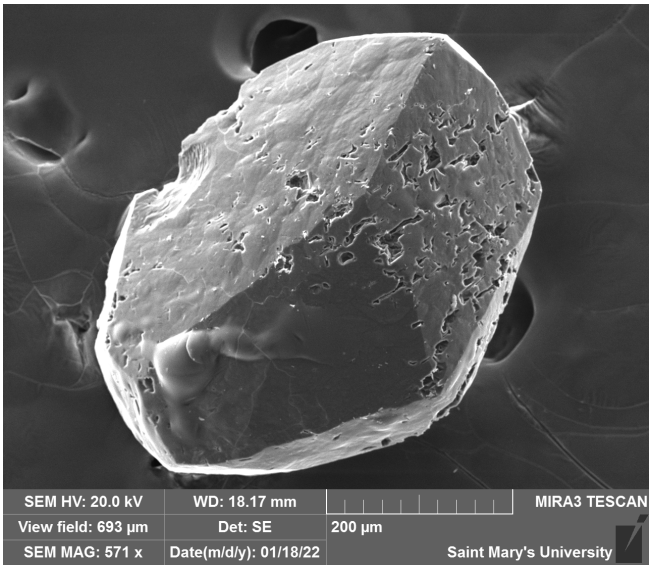

Figure 1.1.4: Image of natural diamond from Ekati diamond mine, demonstrating large rounded hillocks on the left side of the crystal.

The variety in secondary features and morphology of diamonds from different kimberlitic pipes and environments is demonstrated clearly with the Lac de Gras samples, as characterized by Fedortchouk, 2019. Within the Lac de Gras kimberlite field, we see octahedral diamond percentages vary from 1.2% (Arnie and Mark kimberlites) to 86.3% (Beartooth kimberlite). We also see variations in tetrahexahedra (THH) diamonds with percentages ranging from 8% (Beartooth Kimberlite) to 65.4% (Misery Kimberlite). Another good analogy to demonstrate this variety of features, is the Ekati Diamond Mine samples. Although close in locality, variations in

the Ekati diamond mine samples are large. Based on 13 kimberlites, there are three regional varieties in diamond morphology on the Ekati diamond mine property (Gurney, 2004). It is important to understand the contributing factors of this morphology, since it will aid in the characterization of features observed in different kimberlite classes and facies. In this study, we will be focusing on the diamond morphology analysis of secondary features in hypabyssal dykes, and sills. From Fedortchouk 2019; 2010, and Gurney 2004 it's clear that diamonds from hypabyssal kimberlite facies will show different resorption features in class 1 versus class 3 kimberlites. This can be attributed to the fact that dykes and sills never erupted through the kimberlite pipe, and the resorption and dissolution features seen on the diamonds that reside in this lithology, will be a direct result of kimberlitic conditions.

1.3 Previous Experiments

Based on experimental studies by Kozai and Arima 2005 and Zhang et al. 2015 dissolution rates are shown to increase with temperature and decreases with pressure. This furthers the conclusion that dissolution, and therefore secondary diamond surface features, will be affected by temperature and pressure conditions, whether in a laboratory or a kimberlite pipe.

Previous experiments by Zhang, Fedortchouk, and Hanley (2015) have looked at the morphological changes from diamond dissolution in experiments conducted in varying temperatures and pressures with ranges of silica content. The diamond dissolution features analyzed in this study were a proxy for kimberlitic fluid. Conclusions made were that these silica rich melts will create features classically made by water resorption. Higher pressures can be attributed to lower dissolution rates and increased rounding. High pressure environments are less likely to cause the varying morphologies (Gurney, 2004).

Experiments done at 1-1.5Gpa by Fedortchouk, 2019 reveal differences in dissolution features based on experimental melt. In fluid-undersaturated melts we see surface graphitization and irregular cavities. Whereas in water saturated diopside melts with fluids we see development of THH crystal morphology, ditrigonal shapes on the {111} face and negative trigons, terraces, and hillocks. Carbon dioxide rich fluid will lead to more {111} face resorption and create deep-pointed bottom and curved bottom coalescent trigons. With the carbonate rich melt there was more weight loss recorded, but more preservation of the crystal shape. Evidently, carbon atom removal and displacement mechanism are controlled by the solvent composition. At lower

pressures diamonds are in a higher graphite stability region and dissolution is paired closely with graphitization, corrosive features, and slower dissolution. At higher temperatures with a hydrous silicate and carbonatitic melt diamonds will experience dissolution without the presence of graphitization. This indicates that solvent composition will influence morphology and surface features but not dissolution rates.

Experiments conducted between 5.7-7.5GPa and temperatures of 1400-1740C by Khokhryakov and Palyanov (2008) reveal variations in dissolution features based on melt composition. At high pressures, in the region of diamond thermodynamic stability, carbonate rich melts act as a solvent for carbon and allow for recrystallization. From these experiments, diamonds in volatile-free carbonate melts experienced 66% weight loss and in short experiments positive trigon development on the {111} face. In CO_2 containing carbonate melts, weight loss was recorded up to 29%, there was positive trigon development on the {111} face, tetrahexahedra (THH) morphology developed on the diamond edge, and rounded triangular hillocks were seen. In experiments with a carbonate melt containing H_2O, features observed depend on the weight percent of H_2O added. With minimal water (7 wt%) there is positive trigon development on the {111} face, and THH morphology development along crystal edges. With increased water concentrations (>7 wt%) there is step-like negative trigons and ditrigonal plates forming on the {111} faces. Conclusions made from this study indicate that H_2O:CO_2 ratios will control trigon orientation, and the presence of water in the system will be an important factor in the crystal shape changes of the diamond in carbonate and carbonate-silicate melts.

1.4 Kimberlite Pipes

Kimberlite pipes are the result of deep plumes and metasomatic processes exuding through weak zones in the lithosphere (Mitchell, 1986). The process of kimberlite formation begins with continental intra-plate magmatism and are primarily found in ancient cratons, occurring in clusters of similar age and source (Mitchell, 1986). Kimberlites are found throughout the world, with discoveries on all continents and ages ranging from Proterozoic to early Tertiary (Sparks, 2006). In Canada, kimberlites have been found on the Buffalo, Sask, Rae, Hearne, Artic, Slave, and Superior craton (Smith, 2008).

Although the majority of kimberlite pipes can largely be categorized into three types, outlined by Smith 2008. The first is class 1 (figure 1.2.1c), largely described by short-lived

intrusive-extrusive processes each different kimberlite unit observed is associated with separate extrusive/intrusive events. Observed are steep, sharp contacts between these events with the number of different events increasing with depth. This is likely due to most intrusive events not having significant power to reach higher in the pipe. Textures vary within the separate kimberlite units, but the infill of this pipe is primarily composed of hypabyssal kimberlites, tuffistic kimberlites and pyroclastic kimberlites. The next type is class 2 (figure 1.2.1a), the prairie kimberlite type. The host for these pipes is primarily competent Paleozoic sediment. Characteristically these pipes display steep sides and open volcanic features. Based on nested craters and sharp/mixed layers of pyroclastic kimberlites, the formation is associated with separate magma pulses which were expelled from the pipe and then rapidly infilled. The reigning lithology of this type is resedimented volcaniclastics and pyroclastics. The third type is class 3 kimberlite pipes (figure 1.2.1b). These pipes are also associated with open volcanic features, although a larger proportion of its infill is from resedimentation. With class 3 we see rapid infill of pyroclastics although the deepest pyroclastics can be retraced to its own eruption, the later infill at the top of the pipe is a result of infill from other pipes and neighboring sediments. The middle of the pipe is composed of resedimented volcanoclastic kimberlites (RVK) with shallow contacts, indicating several events of resedimentation. This type shows no evidence of separate volcanic events and based on the large emplacement of RVK's a slow infill process is determined.

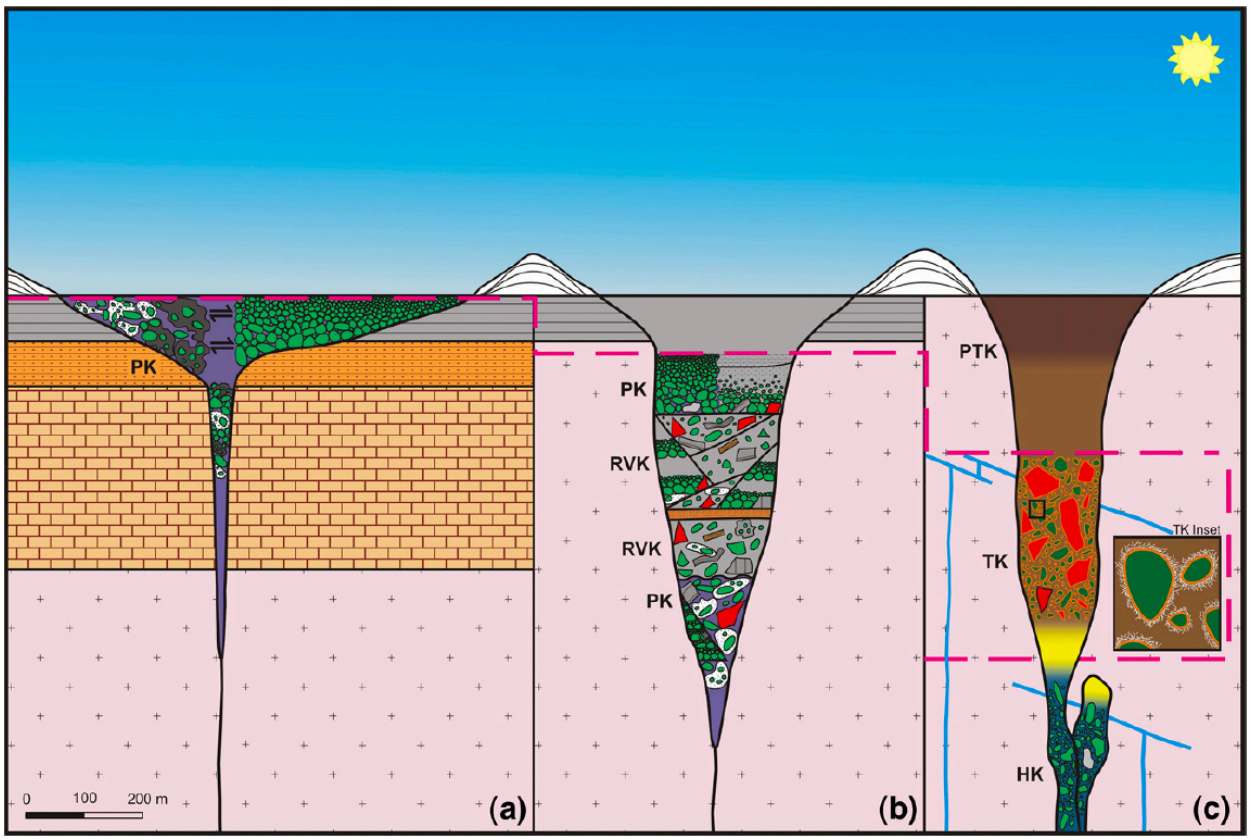

Figure 1.4.1: Visualization of kimberlite class types with facies separation and labels. Facies represented are pyroclastic kimberlites (PK), resedimented volcaniclastic kimberlites (RVK), pyroclastic tuffistic kimberlite (PTK), tuffistic kimberlites (TK) and hypabyssal kimberlites (HK). Three classes are described, from left to right we see class 1, class 3, and then class 2. (Scott Smith, 2008)

1.5 Components of kimberlitic melt and relation to surface features

No kimberlites are created equal, diversity in kimberlite lithology, size, shape and structure could be a result of differences in country rocks (Smith et al. 1999), or composition of volatiles (Skinner and Marsh, 2004). Diamond dissolution features can uncover the effect and degree of these factors through their ability to record the story of the magmatic fluid from the kimberlite pipe in which they ascended (Fedortchouk, 2010). The style and type of resorption features seen depend on the composition of fluids present (Fedortchouk, 2007). Fluid and volatile presence is difficult to determine since contamination can alter volatile concentrations (Fedortchouk, 2010). Two stage flows of melts and gasses can begin very CO_2 rich and then develop into a H_2O dominated fluid during emplacement (Russell et al., 2012). Although CO_2

rich fluids will erase a lot of the {111} diamond face features, if the diamond begins with a CO_2 rich fluid at depth and moves up to a H_2O rich melt, you'll see CO_2 style features on the faces of the diamond and H_2O features along the edges and corners (Fedortchouk, 2010). This complicates kimberlite magma analysis since magma emplacement and kimberlite geology is highly affected by CO_2: H_2O ratios (Fedortchouk, 2010), meaning understanding resultant dissolution features on diamonds, and the conditions under which they occurred is crucial to understanding the evolution of kimberlite lithologies and classes. In Fedortchouk, 2010 natural diamond samples from the Ekati diamond mine kimberlites: Misery, Panda, Beartooth, Koala, Grizzly, Leslie, were analyzed and their surface features categorized based on the kimberlite geology and possible fluid composition. It was found that magma emplacement and kimberlite geology is highly affected by CO2:H2O ratios in the free fluid phase. Within the same pipe, the diamonds showed characteristic resorption features, associated with those kimberlitic conditions. For Misery, Panda and Beartooth diamonds, their smooth surfaces indicated a large amount of free fluid that was H2O rich. The Koala pipe has similar features as noted above, although rarely demonstrated pointy and sharp features. Features of an H2O rich fluid are octahedral into hexoctahedral morphology with little weight loss, ditrigonal shape of the {111} face, few large shallow flat-bottomed trigonal etch pits on the {111} face, well-defined striations along the resorbed edges, circular disks, and preservation of central areas of the diamond with most dissolution occurring along corners and edges (Fedortchouk, 2010). Features of a CO2 rich fluid are preservation of the octahedron shape with more weight loss and {111} faces keeping a trigonal contour, lots of pointed bottom trigon etching and hexagonal pits, thicker and rounder striations, no circular disks, and overwriting of pre-existing features of the face (Fedortchouk, 2010). These descriptions are valid for temperatures of 1150-1350C and 1-7 GPa. Grizzly and Leslie demonstrated sharp characteristics along the diamond edges and sharp regular step-like features, which was unique to these two pipes. These features suggested that Grizzly and Leslie experienced fluid loss in their magma. This is because diamonds can indicate the fluid loss based on their surface features, and even the depth at which this loss occurred (Fedortchouk, 2010). Done through diamond resorption kinetics, if there is highly irregular surface features, complex cavities, and positive trigons, this indicates fluid loss at pressure of ~100kPa, and features similar to the ones seen on most natural kimberlites, with less complex features and more regular surface features, it indicates fluid loss at pressures greater than 1 GPa (Fedortchouk, 2010). Based on

these kinetics (Fedortchouk and Canil, 2009), it was determined that the diamonds had to reside in temperatures above 1200-1300C for hours in order to replicate features similar to the ones seen in Misery, Koala, Panda, and Beartooth and the unique features seen in Grizzly and Leslie, would have been possible if the fluid loss was done at depths greater than 20-30km (Fedortchouk, 2010). This would mean these features developed long before they reached the surface or even, long before the formation of the pipe.

1.6 Correlation of kimberlite lithology and surface features

Diversity in kimberlite lithology, size, shape and structure can be a result of many factors, such as country rocks (Smith et al. 1999) or composition of volatiles (Skinner and Marsh, 2004). Although, the range in resorption features seen in natural diamonds (Robinson, 1979) indicates a large range in dissolution conditions. These dissolution conditions and resultant diamond surface features can not only vary from kimberlite to kimberlite, but can also vary within the same kimberlite, from facies to facies. Conditions of diamond emplacement will depend on the facies in which it is deposited, and since style and type of resorption features seen depend on composition of fluids (Fedortchouk, 2007), obtaining samples from facies can indicate that facies particular emplacement conditions (Fedortchouk, 2017). In a study done by Fedortchouk in 2017, there were four kimberlite lithologies recorded from the Orpa mine in Botswana, a coherent kimberlite from CK-B, a coherent kimberlite from CK-A, a pyroclastic from MVK and an AK15 intrusion, relative placement can be seen in figure 4.1. Lithologies CK-A, CK-B, and MVK all belonged to kimberlite BK1 and AK15 is a separate intrusion. Of the four lithologies, each of their diamond samples demonstrated unique resorption styles. These distinct resorption styles were either present on the majority of diamond, on all rounded diamonds or diamond sides, on all diamonds attached to the kimberlites, or on edges with a combination of resorption styles, in order to ensure that they were kimberlite inherited. The CK-A lithology demonstrated similar resorption to MVK with micro cavities along the diamond edge in the form of linked circular pits, and the presence of groundmass segregation from fluid exsolution indicates fragmentation. The CK-B lithology diamonds were severely corroded, rounded diamonds which resembled diamonds from experiments with carbonate rich melts, no record of fragmentation, and serpentine patches which could potentially be digested xenoliths. The MVK lithology was glossy and well rounded, similar to diamonds under experimental conditions with a high H2O fluid content. The AK15 intrusion had identical style and intensity of

resorption to pyroclastic MVK, but different to CK-A and CK-B. Diamonds from CK-A and CK-B showed strong similarities, the micro cavities in CK-A strongly resembled the ones seen on the corroded surface of B. This indicates that CK-A likely felt the same resorption event that affected CK-B. Based on this study, it is clear that even kimberlite lithologies from the same pipe can experience different emplacement conditions, therefore this must be taken into consideration when analyzing natural diamond data in this paper.

Chapter 2: Methods

2.1 Diamond samples from Ekati mine kimberlites (NWT, Canada)

Natural diamond analysis uses samples from the Ekati diamond mine in the Northwest Territories located in the central slave structural province. Descriptions of the kimberlites are based on Nowicki et al. 2008; 2004. Kimberlites have ages ranging from 45 – 75 Ma (Nowicki et al., 2008; 2004); their depts between 400-600m and surface areas of <3 ha to 20 ha. Kimberlites of the Ekati mine are coherent kimberlites (CK) or volcaniclastic kimberlites (VK)(Nowicki et al., 2008; 2004). Country rocks that host the pipes are Archean granitoids and metamorphed greywacke (Bleeker et al., 1999; Kjarsgaard et al., 2009). No deposition or infill from the phanerozoic or later but there are thin quaternary glacial sediments. Occurrence of mudstone xenoliths from the late cretaceous and tertiary periods within kimberlites indicate surface lithology during the time of kimberlite extrusion (Nowicki et al., 2008; 2004).

Table 2.1.1: Summary of diamonds from kimberlite pipes and their facies used in the SEM study, as well as the total diamond sample count from Ekati, NWT from which the SEM diamonds were selected, based on criteria outlined in section 2.2.

Kimberlite	**Facies**	**# Diamonds**
Anaconda	Hypabyssal	2
Crab	UNK	6
Cub	Volcaniclastic	3
Falcon	UNK	4
Grizzly	Hypabyssal	8
Koala	Crater	22
Lioness	Volcaniclastic	4
Mamba	Crater	2
Misery East	Hypabyssal	2
Pigeon	Crater	3
	Hypabyssal	12
Rat	Crater	3
	SEM Total	105
	Study Total	1363

Diamond samples from CK include diamonds from hypabyssal kimberlites (HK) found as dykes or sills and from pipe-infill coherent kimberlites (pfCK) (Nowicki et al., 2008; 2004). Diamonds from VK include samples from pyroclastic kimberlite (PK), resedimented volcaniclastic kimberlite (RVK), and massive volcaniclastic kimberlite (MVK) (Nowicki et al., 2008; 2004). CK can occur as infill, isolated dykes or minor intrusions in volcanoclastic pipes (Nowicki et al., 2008; 2004). Kimberlite facies differ by the shape of olivine macrocrysts. CK dykes and intrusions have rounded and symmetrical olivine clasts (Nowicki et al., 2008; 2004). CK infill as seen either throughout the entire pipe or in combination with VK displays broken, shard shaped olivine with a large size distribution (Nowicki et al., 2008; 2004).

VK include PK and RVK. PK is coherent fragmental clast supported and olivine rich with coarse grained texture and bedding features (Nowicki et al., 2008; 2004). PK is often found deep in the pipes as either massive bodies or interbedded with other VKs. RVK is present in most of kimberlite pipes of the Ekati mine (Nowicki et al., 2008; 2004). RVK is characteristically composed of single broken and angular olivine grains, a dark and very fine-grained clastic matrix, and with xenoliths of mudstone and host rocks (Nowicki et al., 2008; 2004).

2.2 Natural Diamond Characterization

Natural diamonds were observed and logged on a stereomicroscope and petrographic microscope under reflected light and then those which fit the required criteria were further pictured using a scanning electron microscope (SEM). Samples were logged based on book number, project title, sample name, diamond number, morphology, surface features and whether they displayed kimberlite or mantle features, based on Fedortchouk 2019. The following approach was used:

1. Diamond crystal morphologies were divided into tetrahexahedra (THH), octahedron, fragment, cube.
2. When octahedral {111} faces were present, they were described as ditrigonal or trigonal.
3. The following surface features were observed: hexagonal pits, hillocks, lamellae, negative trigons, circular pits, or square pits.

The selection approach for the diamonds is outlined in figure 2.2.1. First, the diamonds that were either whole or had an unfragmented (<50% breakage) surfaces large enough for analysis were chosen. Diamonds with small or no fragmentation were further divided into diamonds displaying kimberlitic vs. pre-kimberlitic resorption. The following features were used as an indication of kimberlitic resorption:

- rounded corners and edges, a glossy or frosted surface,
- ditrigonal shape of {111}

Selected diamonds which displayed kimberlitic resorption were further divided into:

- diamonds with low-relief surface textures
- corrosion sculptures and other sharp features.

In order to determine the presence of corrosion sculptures, there had to be evidence of channels, pits and cavities, hillocks, frosting, and terraces.

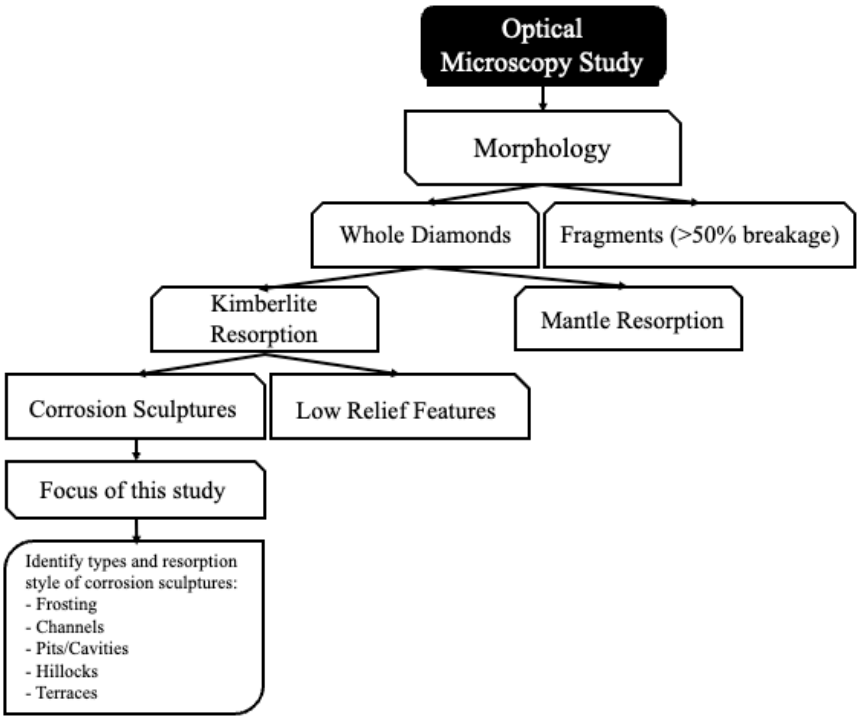

Figure 2.2.1: Workflow of diamond classification used in this study

2.3: Experimental Methods

Experiments used natural octahedral diamonds from Yakutian kimberlites. The diamonds were weighed on a microbalance (+- 0.01mg). All diamond faces were photographed under a petrographic microscope using reflected light. Mixtures were prepared to replicate either a

carbonate rich, silicate rich, or mixed melt. Carbonate was added in the form of calcium carbonate powder, which was stored in an over at 110°C. Silicate was prepared from a starting mixture shown in figure 2.3.1 named RB705-2, which was stored in a desiccator to eliminate water saturation. Deionized water was added using a micro syringe and concentration (0-7 wt%) was based on the composition of the mixture. Platinum/gold capsules were measured out to 5mm lengths and lids were welded on using a Lampert PUK 3 welder in micro mode with a power output of 17%. Capsules were mounted in magnesium oxide ceramic spacers, held together in a graphite furnace, encased in Pyrex with NaCl cell sleeves, seen in figure 2.3.2. Experiments were conducted between 0.5-1 GPa at temperatures between 1,000-1,200°C for periods of 2-18hours, experimental breakdown seen in table 2.3.1.Platinum/gold capsules were packed with 2.5mm of starting mixture. Diamond crystals were placed in the center of the capsule and covered with mixture until 1mm from the top of the capsule. Based on mixture weight, appropriate water content was added, and capsule is sealed with a platinum/gold lid.

Table 2.3.1: Composition of RB705-2 based on weight percent of its various components.

Mixture	**RB705-2 (H_20, 7wt%)**	**RB705-2 (H_20, 5wt%)**
SiO_2	26.26	26.48
TiO_2	3.70	3.92
Al_2O_3	5.70	5.92
Fe_2O_3	10.58	10.80
MgO	5.70	5.93
CaO	24.56	24.78
Na_2O	0.43	0.65
K_2O	2.19	2.41
H_2O	7.00	5.00
CO_2	13.89	14.11
Total	100.00	100.00

Table 2.3.2: Experimental conditions

Run #	Diamond label	Starting composition	Capsule	H2O, wt%	Temperature, °C	Pressure, GPa	Duration, hr
PC-229	RT-1	CaCO3+K2CO3 (1:1)	Pt	0	1000	1	2
PC-237	RT-2	RB705-2	Au-Pd	7%	1200	1	18
PC-237	RT-3	CaCO3	Pt	0	1200	1	18
PC-240	RT-4	RB705-2	Au-Pd	5%	1100	1	18
PC-240	RT-5	CaCO3	Au-Pd	0	1100	1	18
PC-242	RT-6	RB705-2 + CaCO3 (1:1)	Au-Pd	0	1100	1	18
PC-243	RT-7	RB705-2	Au-Pd	5%	1200	0.5	10
PC-243	RT-8	CaCO3	Au-Pd	0	1200	0.5	10

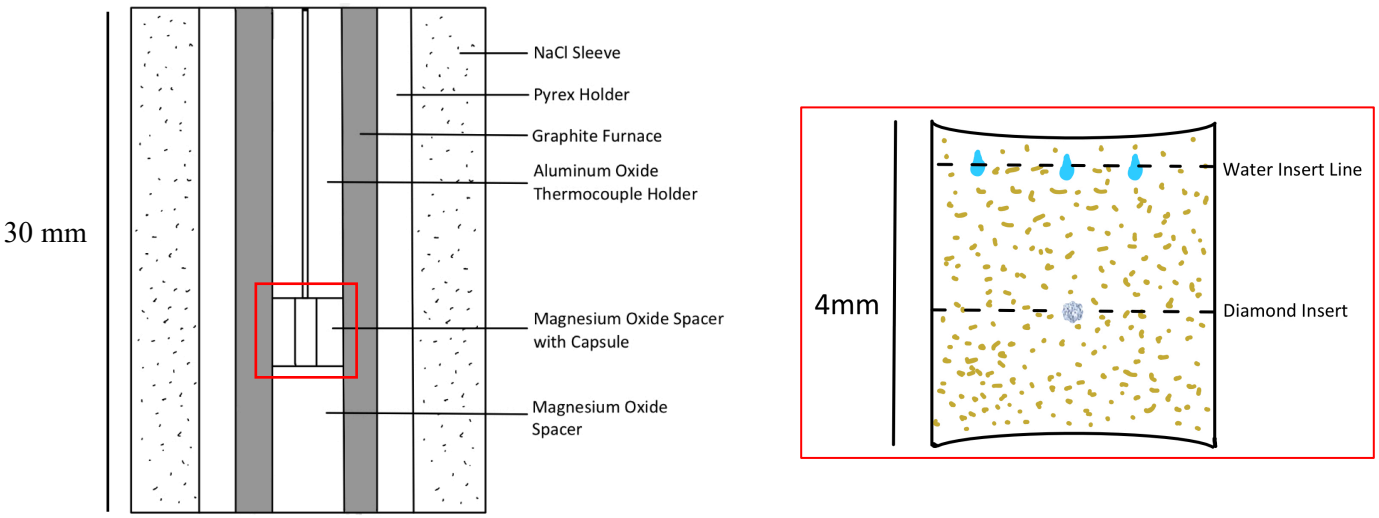

Figure 2.3.1: Configuration of the experimental assembly. Right inlet demonstrates diamond placement within capsule and at which level water was added to mixture.

Experiments were done in a high-pressure piston cylinder apparatus using a pyrex NaCl cell. Assembly was lubricated using lead foil and molybdenum lubricant and then placed inside the bomb. A Al_2O_3 thermocouple holder led two wires of opposite charges to the top of the Au-Pd capsule and were used to measure the temperature in the graphite furnace. Each run began with a slow pressurization to ~0.1 GPa and an increase to 600°C at a rate of 50°/min and held at 600° for 6 minutes. Then the system is pressurized to the desired pressure and the temperature is increased to the final temperature at a rate of 50°/min. Experiment was quenched by the slow elimination of pressure on the bottom piston, temperature being turned off, and then allowed to cool for ~10 minutes before removal from the bomb.

Chapter 3: Results

3.1 Experimental Results

3.1.1 Results at 1000ºC

The first experiment PC-229 was done at 1000ºC at 1GPa of pressure for 2 hours on diamond RT-1. The melt composition was a calcium carbonate and potassium carbonate mix combined in a one-to-one ratio. This experiment yielded negligible results (figure 3.1.1.1). From an optical microscopy analysis there is no surface graphitization observed, no crystal shape deformation and no surface feature development.

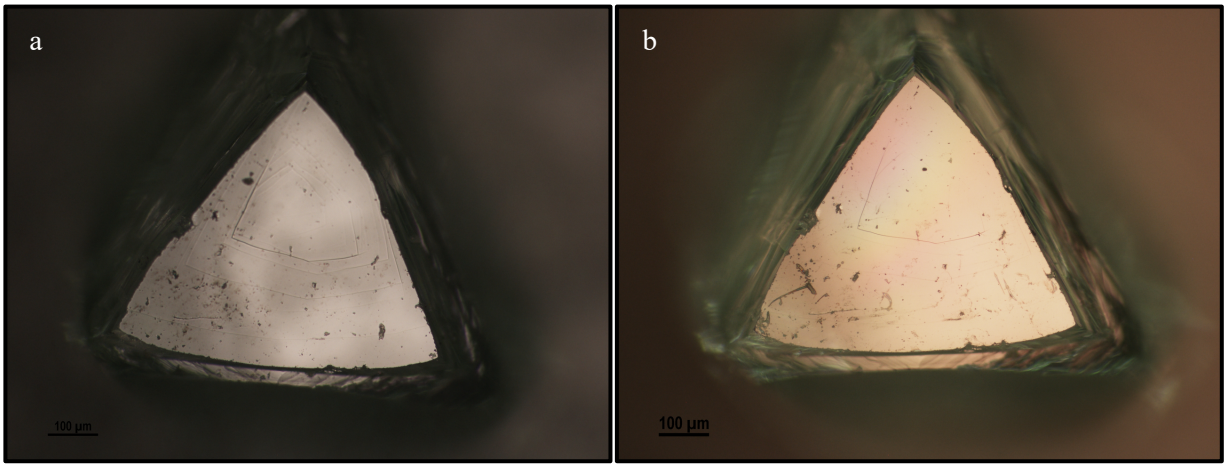

Figure 3.1.1.1: Images of RT-1 before (a) and after (b) experiment, demonstrating little to no change.

3.1.2 Results at 1100ºC

Three runs conducted at 1100C at 1 GPa for 18 hours examined diamond dissolution in a silicate rich melt (RB705-2), carbonate rich melt, and in mixed composition (RB705-2 and CaCO3 in 1:1 ratio). Diamond dissolution in RB705-2 (table 2.3.1) with 5% water by weight percent (diamond RT-4) produced minor, patchy, surface graphitization covering less than 5% of the diamond surface (figure 3.1.2.1). We see moderate rounding along 90% of diamond edges as

the diamond begins to develop several tetrahexahedra surfaces (THH). All diamond faces developed negative trigons, and pre-existing pits and cavities developed into complex features.

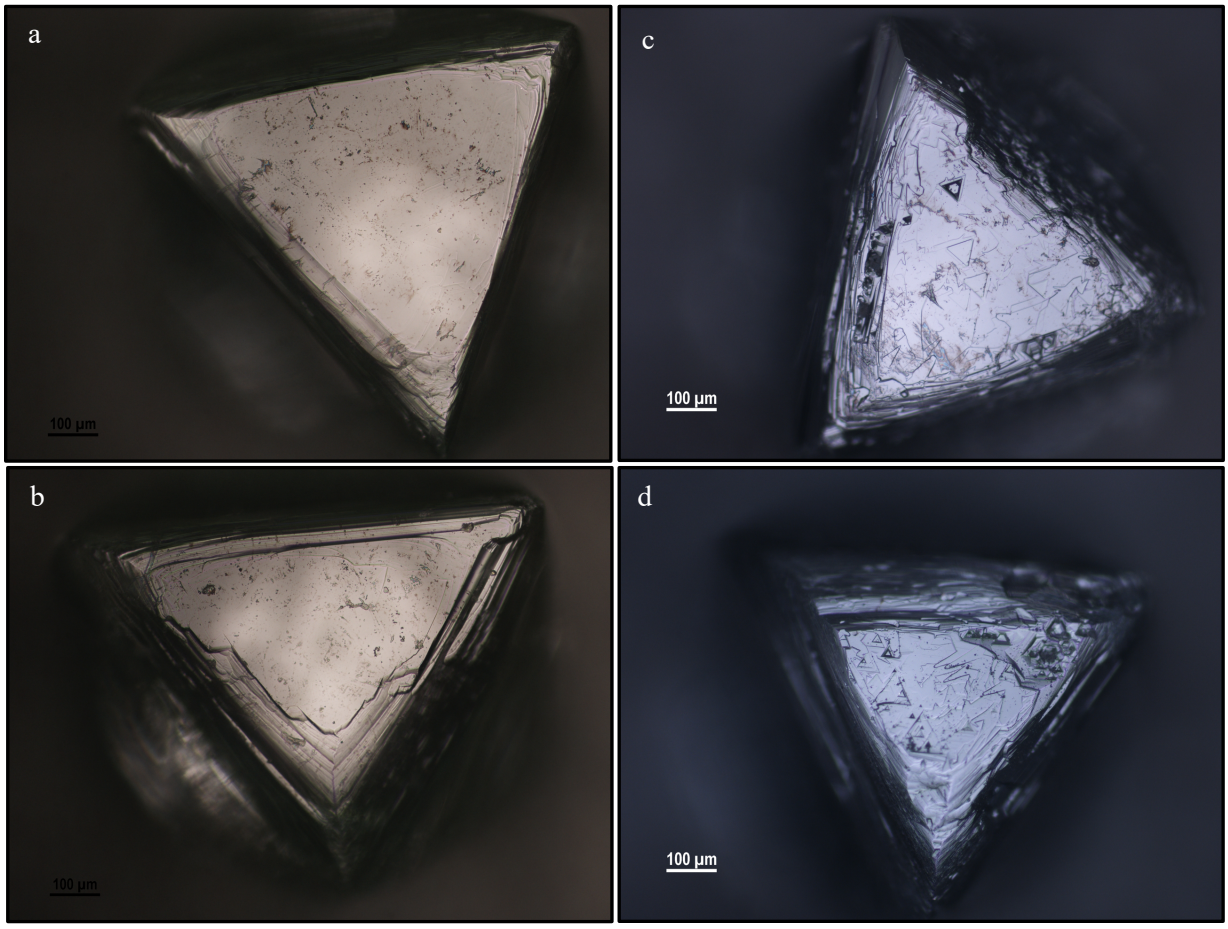

Figure 3.1.2.1: Images of RT-4 from before (a-b) and after (c-d) run PC-240 (c) minor graphitization in bottom left diamond corner and scattered throughout the middle of diamond RT-4, moderate rounding along diamond edges as the beginning of THH morphology development (d) negative trigons with varying depths and sizes and complex features with deep pits in top right corner of diamond.

Diamond (RT-5) dissolution in a carbonate rich melt produced moderate surface graphitization covering approximately 5% of the diamond surface. Under a petrographic microscope using reflected light no crystal shape changes were observed. Early trigon development is seen aligned along terraces (figure 3.1.2.2) and pre-existing pits and cavities of the diamonds. Most trigons were very shallow and no more than 1um in size.

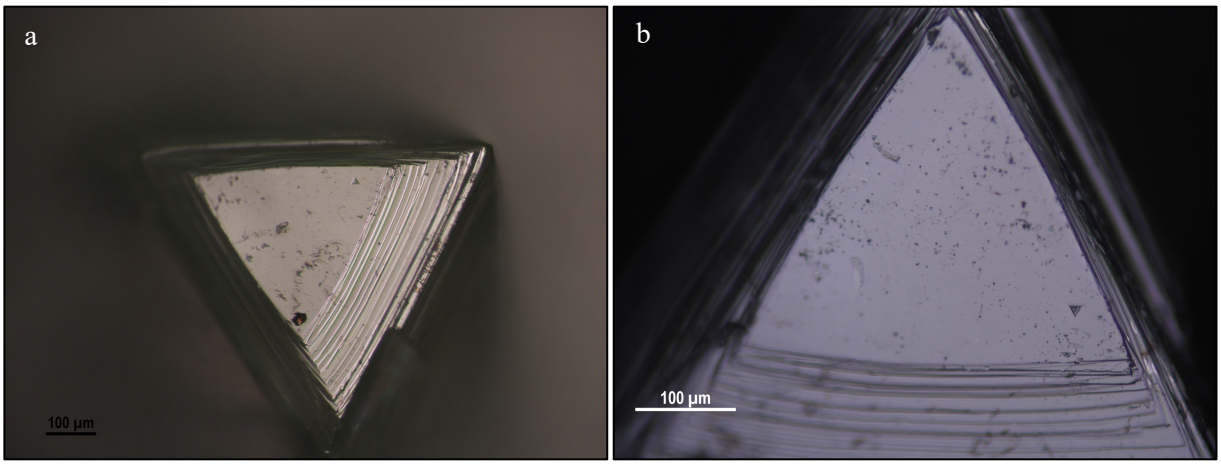

Figure 3.1.2.2: Images of RT-5 before (a) and after (b) run PC-240, seen is the development of negative trigons aligned along low elevation terrace on diamond.

Dissolution in a mix of RB705-2 and $CaCO_3$ (RT-6) in a one-to-one ratio with no water present produced minor surface graphitization, covering less than 5% of the diamond surface. Crystal shape changes were negligible. The most prevalent surface feature development is negative trigons. Pre-experiment no trigons were observed on the diamond face, post-experiment trigons are seen on every side of the diamond surface, ranging in sizes of less than 9um up to 36um, in combination with deep pit development on three faces (Figure 3.1.2.3).

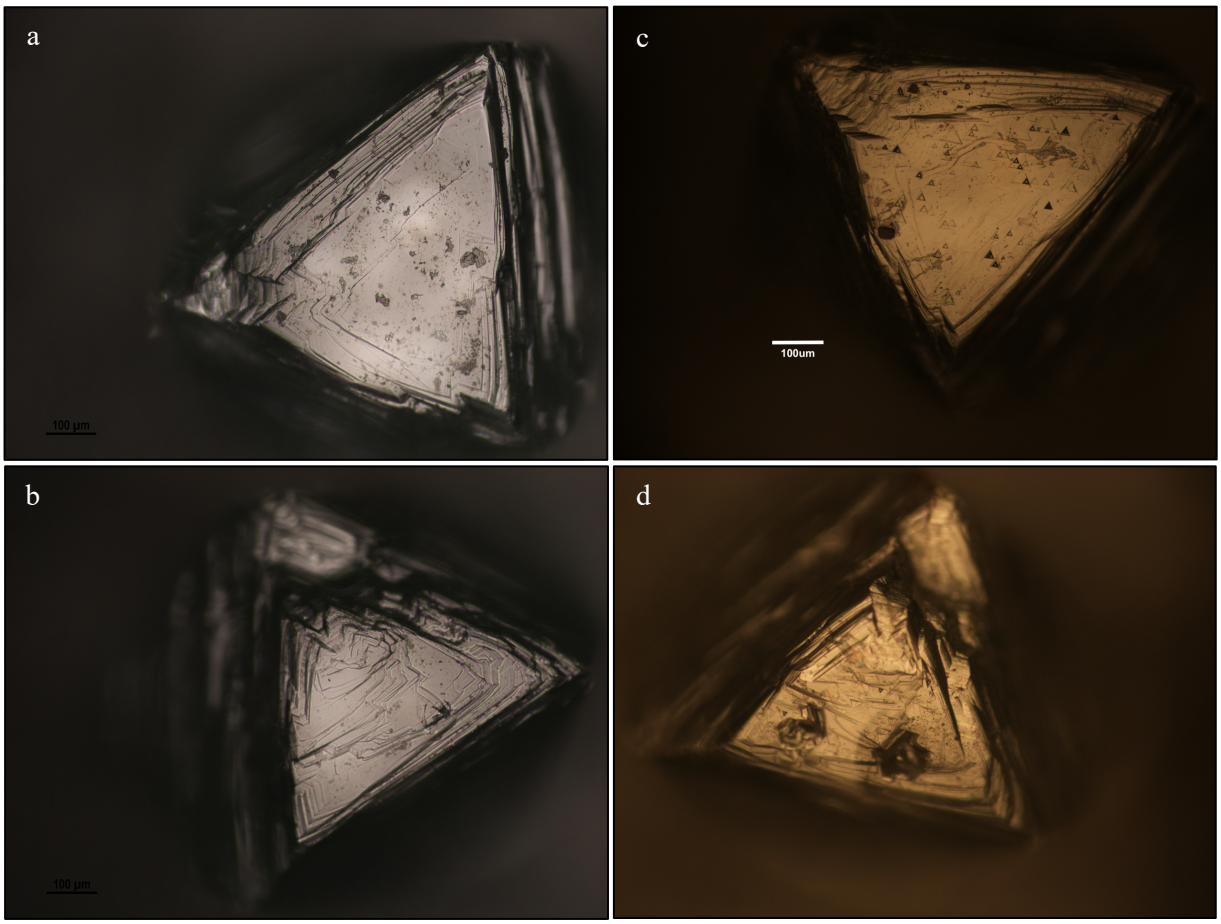

Figure 3.1.2.3: Images of RT-6 from before (a-b) and after (c-d) PC-242, resultant dissolution can be seen in the development of multiple negative trigons (c), and deep pits (d).

3.1.3 Results at 1200C

Diamond dissolution was examined in a carbonate rich melt and a silicate rich melt at 1200C at 0.5 GPa and at 1 GPa. Run PC-237 at 1 GPa using RB705-2 composition with 7wt% water (table 2.3.1) produced no surface graphitization on any side of the diamond. Crystal shape was completely transformed into a rounded THH or dodecahedra shape (figure 3.1.3.1). Changes in crystal shape were accompanied by the development of terraces, hillocks, and frosting. Terraces are seen on every diamond face and contribute greatly to the frosting. Hillocks are round and appear along the diamond's flat surfaces, where the terraces start to taper off.

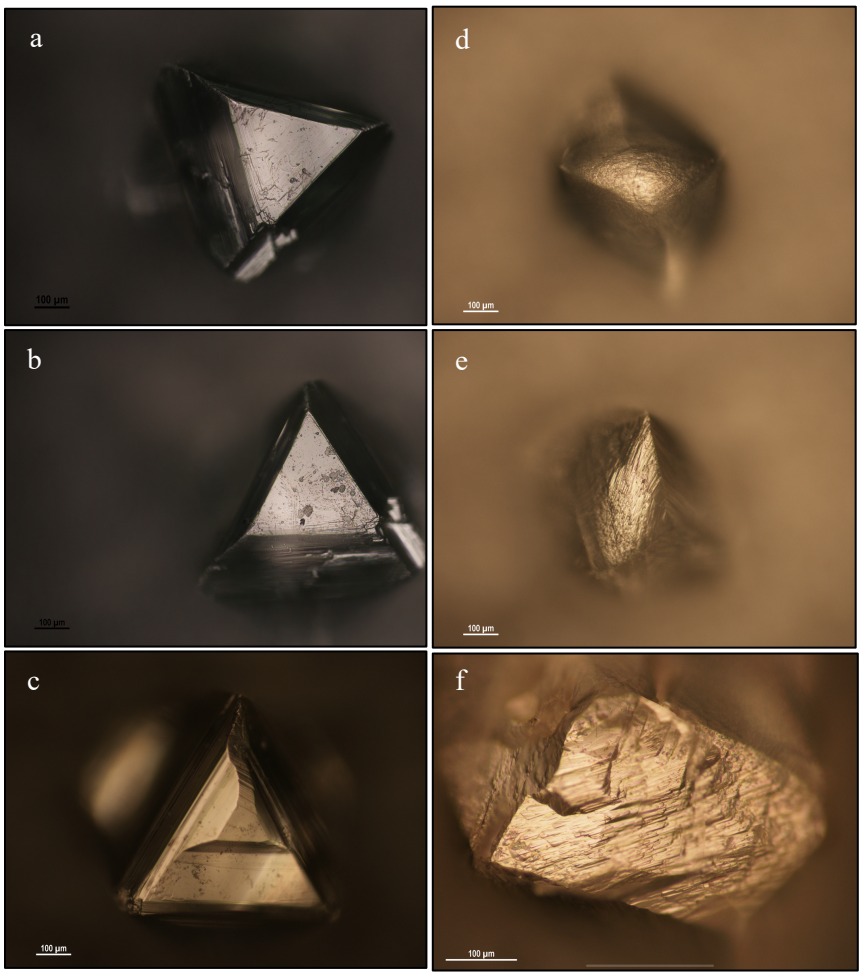

Figure 3.1.3.1: Diamond RT-2 from run PC-237 before (a-c) and after (d-f) completely resorbed and rounded into a THH crystal shape, (d) with small terrace development giving rise to a frosted surface, (e) there is small terrace buildup along the rounded diamond edge, (f) round, large hillocks developed near diamond edge where terraces taper off.

Dissolution of diamond RT-3 at 1 GPa in carbonate rich melt produced extensive surface graphitization covering ~80% of the diamond surface (Figure 3.1.3.2). Crystal shape was not modified significantly enough for any changes to be noted. Surface resorption features produced pits and negative trigons. Pits occur most frequently in regions of high graphitization, as seen in figure 3.1.3.2. There is trigon development on all eight diamond faces, with flat regions of low graphitization having the densest population (figure 3.1.3.3).

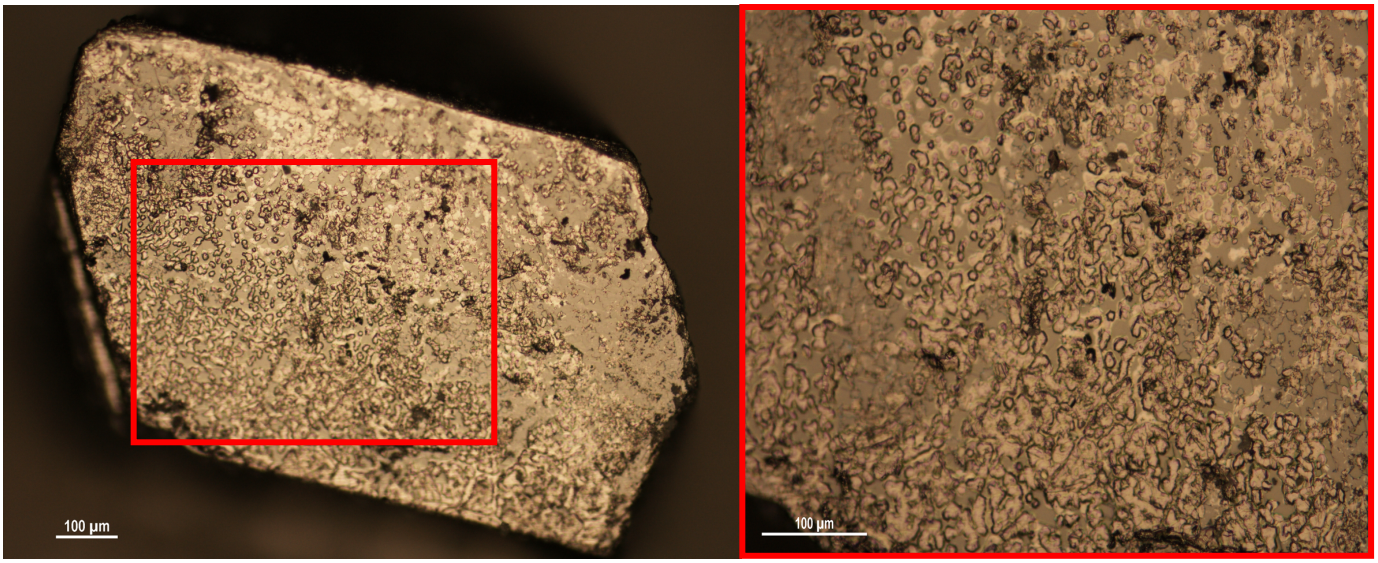

Figure 3.1.3.2: Images of diamond RT-3 from PC-237 demonstrating extensive surface graphitization of diamond face, with right inlet (in red) highlighting small pits developing in region of high graphitization.

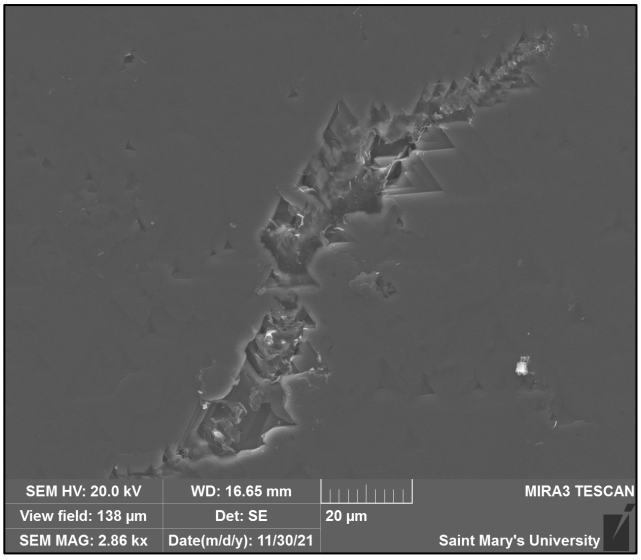

Figure 3.1.3.3: Scanning electron image of RT-3 from PC-237 showing negative trigon development along fracture.

Dissolution at 0.5 GPa of diamond RT-7 in run PC-243 in a silicate rich melt (table 2.3.1) produced minor graphitization seen on less than 5% of the diamond surface, primarily only in regions with complex surface features (figure 3.1.3.4). Crystal shape shows significant transformation due to rounding of crystal edges and giving the diamond a rounded octahedra shape. Surface feature include negative trigons (figure 3 .1.3.4d), deep pits and cavities (figure 3.1.3.4e), and frosting (figure 3.1.3.4f).

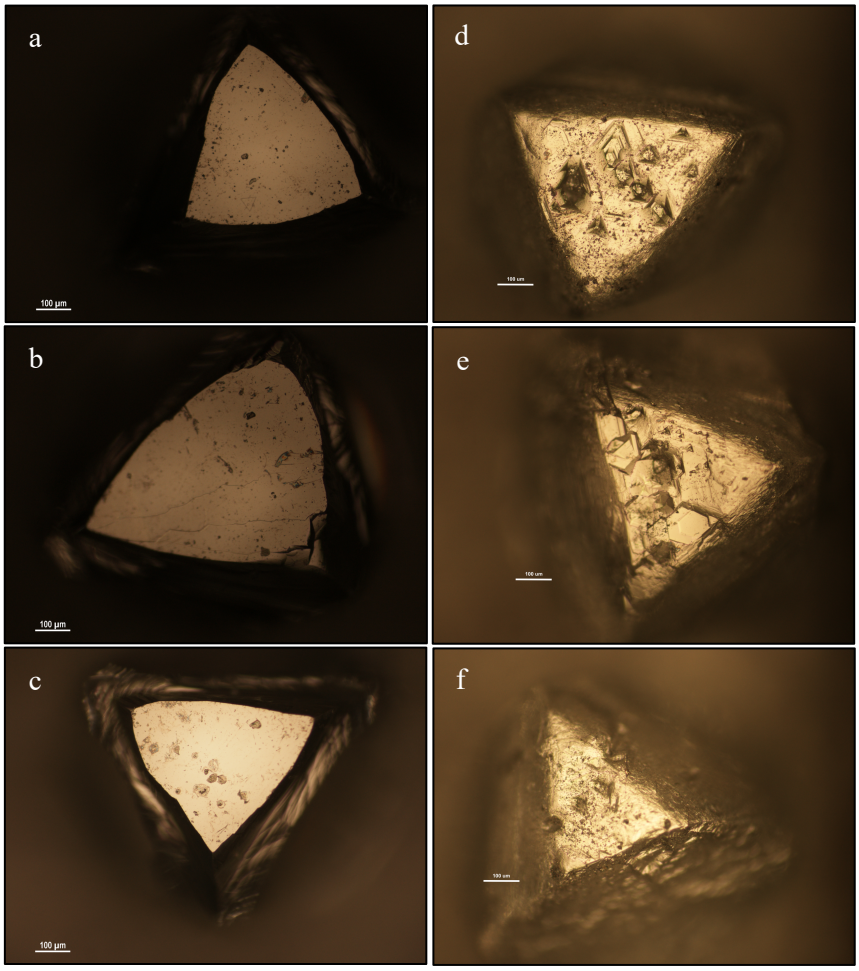

Figure 3.1.3.4: Image of diamond RT-7 before (a-c) and after (d-f) run PC-243 with diamond shows minor surface graphitization, (d-f) rounding along diamond edge, (d) negative trigons, (e) deep hexagonal pits, (f) frosting.

Run PC-243 at 0.5 GPa with a carbonate rich melt, diamond RT-8 has extensive surface graphitization covering more than 80% of the diamond surface (figure 3.1.3.5) and preserved octahedral crystal shape. No rounding was observed along any face, edge or point of the diamond. Very minor surface features are observed, small pits occurring along highly graphitized surfaces of the diamond face (figure 3.1.3.5d).

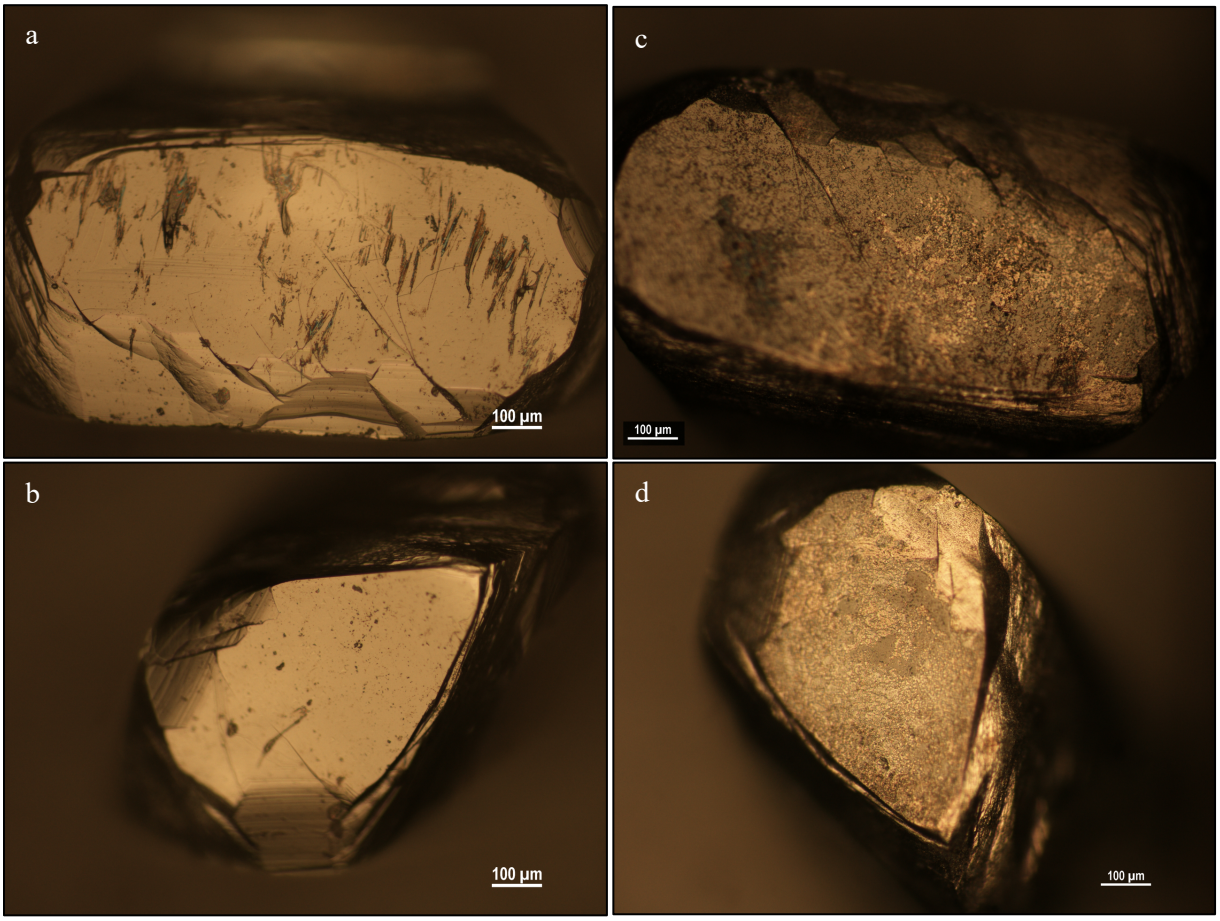

Figure 3.1.3.5: Diamond RT-8 before (a-b) and after (c-d) PC-243, surface graphitization seen on the majority of the diamond surface, (d) small shallow pits developing atop highly graphitized regions.

3.2 Natural Diamond Results

3.2.1 Different resorption types described

Examination of back-scattered electron images revealed four resorption styles on 94 diamonds imaged under SEM (figure 3.2.1.6).

The first resorption style is characterized by small sharp hillocks, aligned along plastic deformation lamellae (figure 3.2.1.1a) and large rounded hillocks scattered along flat regions of the diamond face (figure 3.2.1.1b). In this resorption style more than 50% of the diamond surface is covered in hillocks.

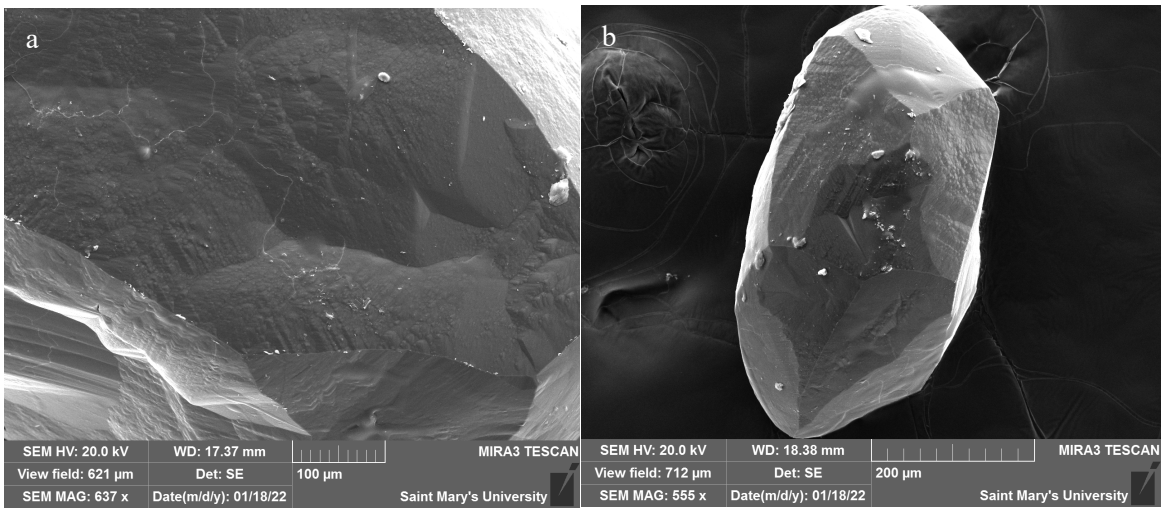

Figure 3.2.1.1: Representative images for resorption type 1 a) small sharp hillocks aligned along the plastic deformation, b) large rounded scattered around areas without plastic deformation.

The second resorption style is recognized by large drop-shapes hillocks (figure 3.2.1.2a), parallel terrace buildup along flat regions of the diamond (figure 3.2.1.2b), and deep channels throughout the inside of the diamond (figure 3.2.1.2b).

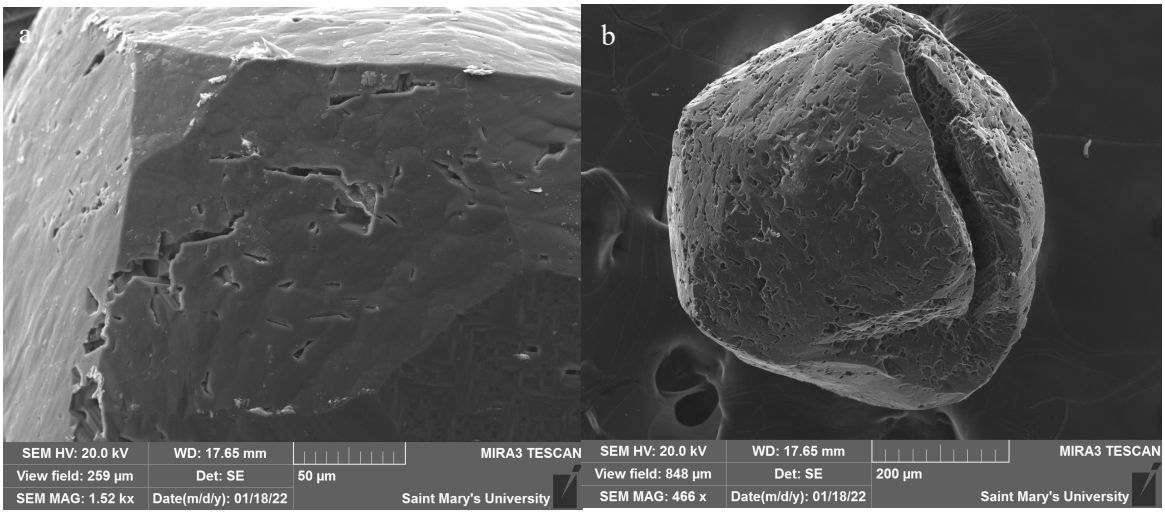

Figure 3.2.1.2: Representative images for resorption style 2 a) parallel terrace buildup along flat faces, b) terraces and large, rounded hillocks.

The third resorption style is characterized by long, parallel terraces which end in round hillocks (figure 3.2.1.3a), as well as small, rounded hillocks, consistently spread along most of the diamond surface (figure 3.2.1.3b). The primary difference between resorption style two and

three are that style two has deep channels throughout the diamond, whereas diamonds from style three do not have these corrosive channels.

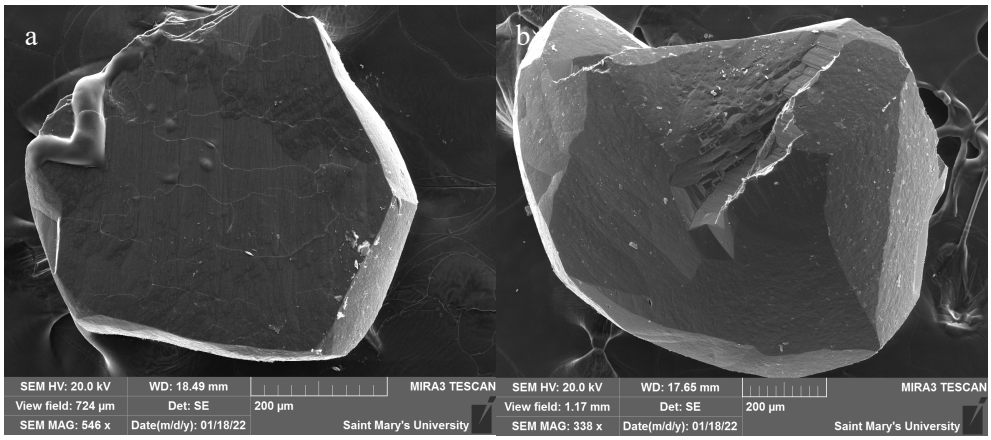

Figure 3.2.1.3: Representative images for resorption style 3 a) long parallel terraces ending in small rounded hillocks, b) spread out small rounded hillocks throughout most of the diamond surface.

The fourth style is characterized by sharp features (figure 3.2.1.4a), islands of smaller sharp hillocks (figure 3.2.1.4b), infrequent large, rounded hillocks, and frosting from sharp terraces (figure 3.2.1.4c).

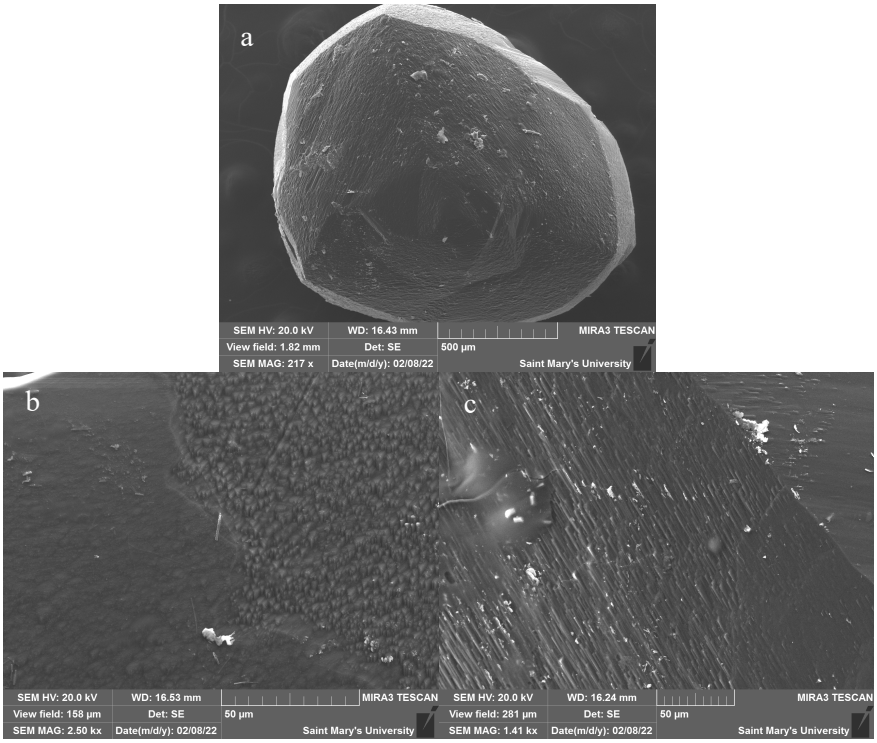

Figure 3.2.1.4: Representative image for resorption style four demonstrating a) sharp corners contributing to frosting, b) islands of differently resorbed regions, c) sharp hillocks.

3.2.2 Relationship between diamond resorption and kimberlite lithology

From the 94 diamonds observed, there were four known kimberlite facies and four different resorption styles detected. The four kimberlite facies for which samples were analyzed is volcaniclastic, resedimented volcaniclastic, crater, and hypabyssal. A summary of how many times each resorption style was seen in each facies is summarized in table 3.2.2.1.

The first resorption style was most common in resedimented volcaniclastic with 5 samples, hypabyssal and volcaniclastic came after with 3 diamonds fitting this resorption style, then crater facies had one diamond which belonged to this style.

With the second resorption style it was only recognized in six diamonds from known lithologies.

The third resorption style was most represented in the crater facies, with 7 diamond samples demonstrating this style. Then we see volcaniclastic with 3 samples in this resorption style, and finally hypabyssal with one sample belonging to this resorption style.

With the fourth resorption style there is the strongest correlation, with the hypabyssal facies having 15 diamonds which demonstrated characteristics of this resorption style. Then volcaniclastic, resedimented volcaniclastic and crater each having 3 samples which belong to this resorption style.

Table 3.2.2.1: Data from diamonds analyzed through electron scanning microscope (SEM). Four resorption styles from four facies were detected from the analysis. Above is the compilation of which resorption styles were detected from the four kimberlite facies.

Kimberlite	Lithology	Diamond studied with SEM	Number of diamonds showing resorption type			
			1	2	3	4
		BR-2				
Cub	Volcaniclastic	CB2-4				
Cub	Volcaniclastic	CB3-1				
Cub	Volcaniclastic	CB3-6				
Crab		CB4-1				
Crab		CR1-4				
Crab		CR1-6				
Crab		CR1-7				
Crab		CR1-8				

Crab		CR2-1				
	RVK	C-1				
	RVK	D-7				
	RVK	F-7				
		F-3				
		F-4				
		F-5				
	RVK	F-8				
	RVK	F-9				
	RVK	B-3				
	RVK	B-6				
	RVK	B-7				
		A-1				
		A-7				
		05#2-4				
		05#2-2				
		27/29-1				
		96-31-25				
		96-31-28				
		96-31-31				
		96-31-34				
Lioness	Volcaniclastic	#02-04-12				
Lioness	Volcaniclastic	#02-04-29				
Lioness	Volcaniclastic	#02-04-30				
Lioness	Volcaniclastic	#02-04-32				
Koala	Crater 1b	K-10-345-4				
Koala	Crater 1b	K-10-345-15				
Koala	Crater 1b	K-10-345-16				
Koala		K-12-345-8				
Koala		K-12-345-16				
Koala		K-12-345-19				
Koala		K-12-345-22				
Koala		K-15-345-1				
Koala		K-15-345-9				
Koala		K-14-345-1				
Koala		K-14-345-7				
Koala		K-14-345-9				
Koala		K-14-345-17				
Koala		K-17-345-2				

Koala		K-17-345-5				
Koala		K-17-345-6				
Koala		K-17-345-20				
Koala		K-13-345-3				
Koala		K-13-345-5				
Koala		K-13-345-7				
Koala		K-13-345-14				
Koala		K-13-345-15				
Pigeon	Hypabyssal	#97-54-1-1				
Pigeon	Hypabyssal	#97-54-1-6				
Pigeon	Hypabyssal	#97-54-1-11				
Pigeon	Hypabyssal	#97-54-1-14				
Pigeon	Hypabyssal	#97-54-1-19				
Pigeon	Hypabyssal	#97-54-1-24				
Pigeon	Hypabyssal	#97-54-1-38				
Pigeon	Hypabyssal	#97-54-2-1				
Pigeon	Hypabyssal	#97-54-2-2				
Pigeon	Hypabyssal	#97-54-2-3				
Pigeon	Hypabyssal	#97-54-2-8				
Pigeon	Hypabyssal	#97-54-2-10				
		93-344CH93-11A				
Anaconda	Hypabyssal	96-17-1				
Anaconda	Hypabyssal	96-17-5				
Misery East	Hypabyssal	MGT-03#1-1				
Misery East	Hypabyssal	MGT-03#1-2				
Grizzly	Hypabyssal	#92-2-2				
Grizzly	Hypabyssal	#92-2-3				
Grizzly	Hypabyssal	#92-2-6				
Grizzly	Hypabyssal	#92-2-7				
Grizzly	Hypabyssal	#92-2-11				
Grizzly	Hypabyssal	#92-2-22				
Grizzly	Hypabyssal	#92-2-35				
Grizzly	Hypabyssal	#92-2-46				
Rat	Crater	RT-1-2				
Rat	Crater	RT-1-3				
Rat	Crater	RT-1-1				
		DDH96-1#2-4				

		DDH96-1#2-5				
		DDH96-06#1-5				
		DDH96-06#1-7				
		DDH96-06#1-8				
		DDH96-07#1-2				
		DDH96-07#1-3				
		DDH96-07#1-5				
		DDH96-07#1-7				
Mamba	Crater	DDH96-8#1-1				
Mamba	Crater	DDH96-8#2-5				
Rattler	Crater (Hypabyssal)	DDH96-13#1-4				
Rattler	Crater (Hypabyssal)	DDH96-13#1-7				
Rattler	Crater (Hypabyssal)	DDH96-13#1-23				
Pigeon	Crater	#97-55-3				
	Crater	#97-55-7				
	Crater	#97-55-14				

Chapter 4: Discussion

4.1 Results from experiments

In alignment with the goal of this study being the characterization of kimberlitic conditions through diamond surface features, experiments were conducted to further understand which conditions can be associated with diamond surface features. The largest experimental factor was starting composition of melt. The focus was to compare carbonate rich melt conditions, silicate rich melt compositions, and a combination of both. From these experiments, there was clear distinctions in end product morphology, etching, and graphitization due to changes in conditions.

Under a carbonate rich environment, there was preservation of the octahedral morphology of the diamond in all samples. In terms of etching, there was trigon development, and minor shallow pits in regions of high graphitization. The diamond at conditions of 1100^{o}C only developed minor etching through small trigons and some pits. The diamonds at 1200^{o}C with a carbonate rich melt both also had minor trigon development, although the etching was more extensive under the higher pressure (1GPa). There was extensive graphitization seen on the diamonds at 0.5 GPa and 1GPa of pressure, at 1200^{o}C. The carbonate rich diamond at 1100^{o}C has very minor graphitization. This could indicate that surface graphitization is more influenced by temperature than pressure conditions.

Under the silicate rich environment, there is moderate to extensive rounding and changes in morphology. In diamond RT-4 at 1100^{o}C at 1GPa there is minor rounding along the crystal edges, with diamond RT-7 at 1200^{o}C at 0.5 GPa there is moderate rounding and slightly more development of THH faces, and with diamond RT-2 at 1200^{o}C at 1 GPa there is extensive rounding, with the diamond being almost completely resorbed to THH morphology. This indicates that there is direct correlation between temperature and pressure and a diamonds morphological evolution towards a THH shape. Although, it should be noted that in RT-2 there was 2wt% higher water content than in RT-4 and RT-7. In terms of diamond etching, all three diamonds became frosted, and had minor trigon development. The deepest and most complex etching was seen in diamond RT-7, RT-2 was the only diamond to develop hillocks and significant terraces, and the etching on RT-4 was mainly low relief and infrequent. Diamond RT-4 was the only one under the silicate rich environment that developed surface graphitization, although it was very minor. It could be hypothesized that the stress on diamond RT-2 and RT-7

was too extensive for the development of surface graphitization, especially in diamond RT-2 where the presence of hillocks indicates great stress was felt by the diamond.

When comparing features seen on diamonds from silicate versus carbonate rich melt the largest differences are seen in the morphological changes, etching and graphitization. Based on experiments silicate melts at or above 1100ºC at 0.5 GPa were the only conditions to induce rounding and development of THH morphology. With frosting, it was only developed in silicate rich compositions at 1200ºC. Deep pit development occured in all diamonds with silicate components present in the melt except for at conditions of 1200ºC at 1 GPa. It can be concluded that under these heightened pressure and temperature conditions, there must have been something disabling the diamond from developing deep and complex features. Significant surface graphitization was only seen on diamonds in a carbonate rich melt that were conducted at 1200ºC. This indicates that surface graphitization is developed in a carbonate rich environment as well as primarily being affected by temperature conditions and not pressure conditions.

Experiments with mixed conditions were conducted on diamond RT-6 and RT-1. RT-1 was conducted in a mix of K2CO3 and CaCO3 at 1000ºC and 1 GPa of pressure. No significant changes were noted on diamond RT-1. Diamond RT-6 was put in 1100ºC at 1 GPa, it saw the development of many shallow negative trigons on all of the faces, and deep pit development in areas with previous fractures. There was no morphological changes in the diamond and it remained an octahedron post-experiment. Based on the results above and comparing to diamonds RT-5 and RT-4 (which most closely resemble the conditions of RT-6, although in different melts), the complex pit development can be associated with the silicate component of the melt. The lack of morphological change could be due to the carbonate, since under silicate rich melt under the same pressure and temperature, rounding was observed. Overall, when present in a mixed melt there was preservation of the morphology, which means the silicate is a non-contributor to the crystal shape changes, there was deep pit develop, possibly from silicate contributions, and there was reworking and etching through previously present fractures and pits, which could possibly be contributed from the carbonate aspect of the melt through carbon reworking.

Evidently, morphology changes, etching and surface graphitization in diamonds is strongly affected by temperature, pressure and melt conditions, and therefore can be used as an indicator for kimberlitic melt conditions in natural diamonds.

4.2 Resorption styles in natural diamonds from Ekati diamond mine sample

The diamonds studied in this paper are from the Ekati diamond mine in the northwest territories. There were 105 diamonds selected for further study, based on the criteria outlined in figure 2.2.1, these were chosen from 1363 diamond samples, most of which did not meet the study requirements. The study requirements were that the diamond be unfragmented (less than 50% breakage) and demonstrate kimberlite resorption with corrosion sculptures. Of the 105 diamonds studied, there were 11 kimberlites represented: Anaconda, Crab, Cub, Falcon, Grizzly, Koala, Lioness, Mamba, Misery East, Pigeon and Rat. From these 11 kimberlites four kimberlite lithologies were represented, volcaniclastic, resedimented volcaniclastic, crater, and hypabyssal. Based on the 105 diamond samples, general trends in resorption styles were determined. There were four major resorption styles found, in which 77% of the diamonds could be classified. It must be noted that these styles are general and vary slightly from lithology to lithology.

Resorption style 1 is characterized by angular hillocks aligned along plastic deformation lamellae. This style of resorption has not yet been recreated in experiments and it is not indicative of low relief features seen typically in volcaniclastics and additionally the plastic deformation indicates high levels of stress. Based on Fedortchouk (2010) these are features typically seen from conditions which are volatile undersaturated, so limited free fluids. There are two causes proposed for this style of resorption. The first is that these features are actually quite similar to those seen in glossy low relief volcaniclastics, but the diamonds were put under a large amount of stress so they formed hillocks and gave a resulting frosted appearance. The second possibility, following Fedortchouk (2010), is that these are not low relief volcaniclastic features but simply features related to melt or normal reaction in an undersaturated volatile environment, but the additional stress and internal defects in the diamond crystal lattice caused the hillocks to align along the deformation lamellae.

Resorption style 2 has characteristic deep channels and large rounded hillocks. These features have not been thoroughly described in papers yet, although they do show THH morphology and kimberlitic resorption. This style of resorption was not found in experiments with fluids but it was seen in experiments in a felsic silicate melt (Jana Kotková, unpublished internal consultation). This indicates that this resorption style could be a result of the diamond

reacting with the melt. Further studies should be conducted in felsic silicate and similar melts to learn more on this resorption type.

The third resorption style is relatively similar to the first and second, although it is without deep channels and deformation lamellae. It is characterized by small, rounded hillocks throughout most of the diamond surface, and parallel terraces. These features have been previously noted as classic features of volcaniclastics (Fedortchouk, 2010). Although not observed in this paper's experiments, they have been found in previous experiments in volatile undersaturated melts (Fedortchouk, 2010). The presence of small hillocks throughout the diamond indicate that this diamond was likely under a relatively large amount of stress.

Resorption style 4 is characterized by sharp features and islands. We see sharp terraces and corners along the diamond edges, as well islands of hillocks, with the shape and style of hillock varying from island to island. The lithologies that had diamonds which fell under this resorption style were some resedimented volcaniclastic, but primarily hypabyssal and crater. The kimberlite pipe with the most diamonds belonging to this resorption style was Grizzly. This is in alignment with data from Fedortchouk (2010). The cause for these features is proposed to be a fluid deficient environment (Fedortchouk, 2010). The islands with surface features different than their surroundings could be a result of two phases of reaction, or bubbles on the diamonds surface which created a separate environment of dissolution, so that this region of the diamond underwent a different reaction. In Fedortchouk, 2010 these features were only found in Grizzly and Leslie pipes from Ekati, although I found evidence that this resorption style may also be seen in Anaconda, Lioness, Cub, Koala, Pigeon, and Mamba.

4.3 Correlation of kimberlite lithology and surface features in natural diamonds

Based on the four resorption styles demonstrated in the diamonds run under SEM, there were light correlations between the kimberlite lithology and the resorption style seen. With resedimented volcaniclastics from the C to F series of diamonds (same kimberlite), we see a strong correlation with the first resorption style with 80% of the diamonds analyzed, fitting into the first resorption style. With the crater lithology (K-10 to K-17) there is a correlation to the third resorption style, with 66% of the diamonds with an identified resorption style belonging to the third resorption type. The hypabyssal lithology from the pigeon kimberlite saw a light trend towards resorption style four. Of the diamonds with identifiable resorption styles, 62.5% of them

belonged to the four-resorption type. The hypabyssal lithology in the Anaconda, Misery East, and Grizzly kimberlites were all strongly correlated to the fourth resorption style. All the diamonds from hypabyssal lithologies from these kimberlites demonstrated resorption styles that fell into category four. For the crater lithology of the pigeon kimberlite, there was a strong correlation to a particular resorption style and all diamonds analyzed under SEM fell under this resorption style.

Chapter 5: Conclusions

5.1 Conclusions from experimental data

The basis of the experimental work done in this paper was to classify which dissolution features will arise when there are known conditions. The largest differentiating factor in the experiments was melt composition: either carbonate or silicate rich. From these experiments it is determined that carbonate rich melts will preserve octahedral morphology and the trigonal face shape of the diamond, there will be extensive graphitization with pressures larger than 0.5GPa at 1200^{o}C, there will be minor graphitization at 1100^{o}C, and there will be trigon development between 1000-1200^{o}C. These results indicate that graphitization has a stronger correlation with temperature than pressure and will be a direct result of carbonate presence in a melt. From experiments in a silicate rich melt, rounding will occur at temperatures above 1100^{o}C, although extent of rounding grows exponentially at 1200^{o}C. This indicates that silicate presence in a melt will have a large effect on a diamonds shape and morphology. Additionally, in a silicate melt, the most complex and deep pits were developed at a temperature of 1200^{o}C. Indicating that complex feature development with be more influenced by temperature than pressure changes. In conditions of mixed melt, surface features were a combination of what is seen in a carbonate rich melt and a silicate rich melt. The mix was done at 1100^{o}C at 1GPa of pressure. At this temperature in the silicate melt there was minor rounding of the diamond, but under mixed conditions there was no rounding noticed, in a silicate rich melt there were shallow pit development, whereas in mixed conditions the pits and trigons were deeper and more complex. This could indicate that the presence of carbonate in the mixed melt caused these pits to grow deeper into the diamond crystal lattice, as well as limit the diamond rounding. At the same temperature in a carbonate dominated melt, there was negligible trigon development but in the mixed conditions there was trigons seen on every diamond face. These results indicate that when mixed the silicate and carbonate melts will create features different than the ones seen when they are run isolated.

5.2 Conclusions from natural diamond analysis

From the natural diamond analysis, the variety of resorption features indicate that even within similar kimberlites, different lithologies can cause varieties in diamond surface features and resorption styles. The goal of the study was to correlate features seen in the hypabyssal

kimberlite facies, and this was the facies which showed the strongest inclination towards a particular style. From the kimberlites studied, all class 3, it can be said that the hypabyssal lithologies of class 3 kimberlites will have a strong inclination towards sharp features and two phases of reactions, and the kimberlitic melt condition of this facies has a high probability of being fluid deficient.

5.3 Recommendations for future studies

Based on this study, there are many opportunities for further research. The first recommendation would be to further evaluate the relationship between various components in a melt. From the mixed melt experiment, the different components of the melt seemed to influence what surface features were classically seen when these two components were run separately. Further studies should focus on these interactions and how the separate components may overprint or counteract each other, as it would create a better proxy for kimberlitic melt. Another recommendation would be to further investigate class 1 and class 3 hypabyssal melts. There is a trend in resorption style in diamonds from hypabyssal lithologies in class 3 kimberlites, but the evidence proposed in this paper is not substantial enough to draw strong conclusion. Further experiments should be done in fluid deficient settings in order to better replicate the conditions of the class 3 hypabyssal kimberlites.

References

Arima, M. and Kozai, Y. 2008. Diamond dissolution rates in kimberlitic melts at 1300–1500ºC in the graphite stability field. Eur. J. Mineral. 20, 357–364.

Bleeker, W., Ketchum, J., Jackson, V., Villeneuve, M. 1999. The central slave basement complex, Part 1: its structural topology and autochthonous cover. Canadian Journal of Earth Sciences 36(7): 1083-1109.

Fedourtchouk, Y., Canil D. 2009. Diamond oxidation at atmospheric pressure: development of surface features and the effect of oxygen fugacity. Eur. J. Mineral. 21: 623–635.

Fedortchouk, Y., Canil, D., Semenets, E., 2007. Mechanisms of diamond oxidation and their bearing on the fluid composition in kimberlite magmas. Am. Mineral. 92, 1200–1212.

Fedortchouk, Y., Chinn, I.L., Kopylova, M.G., 2017a. Three styles of diamond resorption in a single kimberlite: Effects of volcanic degassing and assimilation. Geology 45, 871–874.

Fedortchouk, Y., Liebske, C., McCammon, C., 2019. Diamond destruction and growth during mantle metasomatism: an experimental study of diamond resorption features. Earth Planet. Sci. Lett. 506, 493–506.

Fedortchouk, Y., Matveev, S., Carlson, J.A., 2010. H2O and CO2 in kimberlitic fluid as recorded by diamonds and olivines in several Ekati Diamond Mine kimberlites, Northwest Territories, Canada. Earth Planet. Sci. Lett. 289, 549–559.

Fedortchouk, Y. and Zhang, Z. 2011. Diamond resorption: link to metasomatic events in the mantle or record of magmatic fluid in kimberlitic magma? The Canadian Mineralogist, 49, 707–719.

Fedortchouk, Y. 2015. Diamond resorption features as a new methods for examining conditions of kimberlite emplacement. Contrib. Mineral. Pertrol. 170, 36.

Field, M. & Scott Smith, B. H., 1998. Textural and genetic classification schemes for kimberlites: a new perspective. In International Kimberlite Conference: Extended Abstracts, Vol. 7, pp. 214-216.

Gurney J.J., Hildebrand, P.R., Carlson, J.A., Fedortchouk, Y., and Dyck, D.R. 2004. The

morphological characterstics of diamonds from the Ekati property, Northwest Territories, Canada. Lithos, 77, 21–38.

Khokhryakov, A.F., Pal'yanov, Y.N., 2007. The evolution of diamond morphology in the process of dissolution: Experimental data. American Mineralogist 92, 909–917.

Kjarsgaard, B. A., Pearson, et al., 2009). Geochemistry of hypabyssal kimberlites from Lac de Gras, Canada: comparisons to a global database and applications to the parent magma problem. Lithos, 112, 236-248.

Kozai, Y. and Arima, M. 2005. Experimental study on diamond dissolution in kimberlitic and lamproitic melts at 1300–1420ºC GPa with controlled oxygen partial pressure. American Mineralogist, 90, 1759–1766.

Mitchell, R.H. 1986. Kimberlites: Mineralogy, Geochemistry, and Petrology. Plenum Press, New York and London.

Nowicki, T., Porritt, L., Crawford, B., Kjarsgaard, B., 2008. Geochemical trends in kimberlites of the Ekati property, Northwest Territories, Canada: Insights on volcanic and resedimentation processes. J. Volcanol. Geotherm. Res. 174, 117–127.

Nowicki, T., Crawford, B., Dyck, D., Carlson, J., McElroy, R., Oshust, P., Helmstaedt, H., 2004. The geology of kimberlite pipes of the Ekati property, Northwest Territories, Canada. Lithos 76, 1–27.

Robinson, D.N. 1979. Surface Textures and Other Features of Diamonds. Ph.D. thesis, 206 pp., University of Cape Town at Cape Town, December.

Russell, J.K., Porritt, L.A., Lavallee, Y., Dingwell, D.B., 2012. Kimberlite ascent by assimilation-fuelled buoyancy. Nature 481, 352–356.

Scott Smith, B. H., 2008. Canadian kimberlites: geological characteristics relevant to emplacement. Journal of Volcanology and Geothermal Research, 174, pp. 9-19.

Sparks, R.S.J., 2013. Kimberlite volcanism. Ann. Rev. Earth Planet. Sci. 41, 497–528.

Skinner, E. M. W., & Marsh, J. S., 2004. Distinct kimberlite pipe classes with contrasting eruption processes. Lithos, 76, pp. 183-200.

Sunagawa, I., 1984. Morphology of natural and synthetic diamond crystals. In: Sunagawa, I. (Ed.), Materials Science of the Earth's Interior. Terra Scientific Publishing, Tokyo, Japan, pp. 303–330.

Tappert, R. and Tappert, M.C. 2011. Diamonds in Nature: A Guide to Rough Diamonds. Springer-Verlag, Berlin Heidelberg.

Tolansky, S., 1968. Graphitized natural diamond. Diamond Res. 8–10.

Wagner, P.A., 1914. Note on graphite-coated diamonds from the Premier Mine. Trans. Geol. Soc. S. Afr. 17, 29–30.

Zhang, Z., Fedortchouk, Y., and Hanley, J. 2015. Evolution of diamond resorption in a silicic aqueous melt at 1-3 GPa: application to kimberlite emplacement and mantle metasomatism. LITHOS.